THE JOURNAL OF BIOLOGICAL CHEMISTRY VOL. 288, NO. 50, pp. 35703–35713, December 13, 2013

Box C/D Small Nucleolar RNA (snoRNA) U60 Regulates Intracellular Cholesterol Trafficking*[S]

Received for publication, May 24, 2013, and in revised form, October 28, 2013 Published, JBC Papers in Press, October 30, 2013, DOI 10.1074/jbc.M113.488577

Katrina A. Brandis[1], Sarah Gale, Sarah Jinn, Stephen J. Langmade, Nicole Dudley-Rucker, Hui Jiang, Rohini Sidhu, Aileen Ren, Anna Goldberg, Jean E. Schaffer, and Daniel S. Ory[2]

From the Diabetic Cardiovascular Disease Center, Washington University School of Medicine, St. Louis, Missouri 63110

Background: The mechanisms regulating internalization of plasma membrane cholesterol in mammalian cells are not well understood.
Results: A cell line haploinsufficient for U60 snoRNA expression exhibits impaired plasma membrane to ER cholesterol trafficking and increased *de novo* cholesterol synthesis.
Conclusion: U60 snoRNA expression regulates cholesterol homeostasis by affecting internalization of plasma membrane cholesterol.
Significance: This is the first study to implicate a snoRNA in regulation of cholesterol homeostasis.

Mobilization of plasma membrane (PM) cholesterol to the endoplasmic reticulum is essential for cellular cholesterol homeostasis. The mechanisms regulating this retrograde, intermembrane cholesterol transfer are not well understood. Because mutant cells with defects in PM to endoplasmic reticulum cholesterol trafficking can be isolated on the basis of resistance to amphotericin B, we conducted an amphotericin B loss-of-function screen in Chinese hamster ovary (CHO) cells using insertional mutagenesis to identify genes that regulate this trafficking mechanism. Mutant line A1 displayed reduced cholesteryl ester formation from PM-derived cholesterol and increased *de novo* cholesterol synthesis, indicating a deficiency in retrograde cholesterol transport. Genotypic analysis revealed that the A1 cell line contained one disrupted allele of the U60 small nucleolar RNA (snoRNA) host gene, resulting in haploinsufficiency of the box C/D snoRNA U60. Complementation and mutational studies revealed the U60 snoRNA to be the essential feature from this locus that affects cholesterol trafficking. Lack of alteration in predicted U60-mediated site-directed methylation of 28 S rRNA in the A1 mutant suggests that the U60 snoRNA modulates cholesterol trafficking by a mechanism that is independent of this canonical function. Our study adds to a growing body of evidence for participation of small noncoding RNAs in cholesterol homeostasis and is the first to implicate a snoRNA in this cellular function.

Cholesterol homeostasis serves to maintain optimal sterol content in mammalian cell membranes. In addition to contributing to the structural properties of the phospholipid bilayer, cholesterol is necessary to maintain plasma membrane (PM)[3] lipid raft structures that house a multitude of integral and membrane-associated proteins and complexes that are critical for cellular function. Cellular cholesterol originates from two sources: low density lipoprotein (LDL)-associated cholesterol and *de novo* synthesis, although uptake of cholesterol through the LDL-receptor pathway is the most quantitatively important of these in mammalian cells under physiological conditions.

The itinerary of LDL-derived cholesterol is well established. Following internalization via the LDL receptor, LDL particles are trafficked to a late endocytic compartment where esters are hydrolyzed by acid lipase to free cholesterol and subsequently released from endolysosomes via the concerted actions of the Niemann-Pick C1 (NPC1)/Niemann-Pick C2 (NPC2) proteins. Most of this cholesterol is then transported to the PM with a minor amount transported directly to the endoplasmic reticulum (ER), Golgi, and mitochondria (1–3). In mammalian cells, the PM is estimated to contain 60–90% of total cellular cholesterol, whereas the ER contains as little as 0.1–2% (4). This steep gradient is maintained despite a brisk flow of cholesterol between these compartments (5). It is hypothesized that this pathway provides for "sampling" of cellular cholesterol levels in the ER, where the sterol-sensing SREBP cleavage-activating protein (SCAP) senses ER cholesterol levels that govern maturation of the sterol regulatory element-binding protein (SREBP) transcription factors, master regulators of genes involved in cholesterol synthesis and uptake.

A number of stimuli influence PM to ER retrograde cholesterol transport, including alteration of PM phospholipid content, insertion of membrane-disordering oxysterols, disruption of lipid rafts, and increasing bulk PM cholesterol content (6–8). Although the mechanism by which cholesterol is transported between the PM and ER membranes is not yet established, it is thought to be nonvesicular in nature (9). Consistent with a protein-mediated mechanism, knockdown of ORP1/2, members of

* This work was supported, in whole or in part, by National Institutes of Health Grants HL1033001 (to D. S. O.) and DK064989 (to J. E. S.).
[S] This article contains supplemental Fig. 1 and Table 1.
[1] Supported by National Institutes of Health Training Grant T32 HL07275.
[2] To whom correspondence should be addressed: Diabetic Cardiovascular Disease Center, Washington University School of Medicine, Box 8086, 660 S. Euclid Ave., St. Louis, MO 63110. Tel.: 314-747-0677; Fax: 314-747-0264, E-mail: dory@wustl.edu.
[3] The abbreviations used are: PM, plasma membrane; snoRNA, small nucleolar RNA; snoRNP, small nucleolar ribonucleoprotein; ER, endoplasmic reticulum; SREBP, sterol regulatory element-binding protein; CE, cholesteryl ester(s); ACAT, acyl-CoA:cholesterol acyltransferase; LPDS, lipoprotein-deficient serum; PC, phosphatidylcholine; LPC, lysophosphatidylcholine; DMSO, dimethyl sulfoxide; RACE, rapid amplification of cDNA ends; qPCR, quantitative PCR; ASE, antisense element.

the oxysterol binding protein family known to participate in intermembrane trafficking of sterols, reduced PM to ER cholesterol trafficking in HeLa cells (10). Likewise, the STARD4 protein has been implicated in intermembrane transfer of cholesterol between the endocytic recycling compartment and ER (11). On the other hand, cholesterol transfer has been shown to occur between closely apposed PM and ER membrane contact sites (12). Although both types of mechanisms may contribute to total retrograde cholesterol transport, their respective contributions under physiologic conditions is uncertain.

In a previous genetic screen, cells selected for resistance to amphotericin B, a cholesterol-dependent pore-forming toxin, isolated mutants from two complementation groups: those harboring defects in transport of cholesterol from the lysosome to the PM and those with defective PM to ER trafficking (13–15). Subsequent studies revealed that former mutants (2-2 and 4-4) resulted from disruption of the *NPC1* gene (16), whereas the genetic defect in the latter mutant (3–6) remains uncharacterized, highlighting the challenge of identification of the mutagenized loci in these ethyl methanesulfonate-generated cell lines (15). Together with molecular simulations and model membrane studies that suggest the availability of cholesterol to trafficking mechanisms may first be determined by its local membrane lipid environment (6, 17, 18), these data raise the possibility that amphotericin B resistance could arise from changes in PM phospholipid content that alter PM cholesterol levels or organization (15). To further delineate the genes involved in the internalization of PM cholesterol, we performed a loss-of-function screen in Chinese hamster ovary (CHO) cells mutagenized with the ROSAβGEO promoter trap virus to isolate mutants resistant to the amphotericin B cholesterol binding toxin (19, 20). Herein, we describe a CHO cell mutant in which a genetic disruption of the U60 small nucleolar RNA (snoRNA) host gene impairs PM to ER retrograde cholesterol transport.

EXPERIMENTAL PROCEDURES

DNA Constructs—For expression of the genomic mouse U60snhg locus, the genomic sequence, including 2 kb of upstream promoter sequence and 1 kb of downstream sequence, was cloned into the pSilencer 4.1-CMV Hygro vector, with CMV and other vector expression sequences removed. A QuikChange II site-directed mutagenesis kit (Stratagene) was used to create mutD and mutASE snoRNA mutant constructs. FLAG epitope-labeled Nop56 (FLAG-Nop56) and FLAG-fibrillarin genes were cloned into the pSilencer 4.1-CMV Hygro vector, with expression driven by the CMV promoter.

Cell Culture—Chinese hamster ovary-K1 (CHO-K1) cells (CRL-9618) were obtained from ATCC. CHO-K1 Cells were maintained in monolayer culture at 37 °C with 5% CO_2. All CHO-derived cell lines were maintained in normal medium consisting of 1:1 Dulbecco's modified Eagle's medium:Ham's F-12, 5% (v/v) fetal calf serum, 2 mM glutamine, 50 units/ml penicillin, 50 μg/ml streptomycin. NIH 3T3 cells (ATCC CRL 1658) were grown in DMEM containing 10% (v/v) calf serum (Sigma) and 50 units/ml penicillin and streptomycin.

Amphotericin B Loss-of-Function Screen—A stable pool of ROSAβGEO-transduced CHO cell mutants was generated as described previously (19). This pool of mutants was grown for 24 h in cholesterol starvation medium consisting of 1:1 DMEM: Ham's F-12 with 1% (v/v) lipoprotein-deficient serum (LPDS), 2 mM glutamine, 50 units/ml penicillin, 50 μg/ml streptomycin, 20 μM lovastatin, and 50 μM mevalonate. Final concentration of DMSO during selection was <1%. Cells were re-fed with 9 μg/ml LDL in 5% LPDS for 24 h. Cells were then treated with 175 μg/ml amphotericin B in DMSO for 6 h and then replaced with normal medium. After recovery, the starvation, LDL treatment, and amphotericin selection were repeated. The surviving mutant CHO cell population was plated at a limiting dilution to select stable amphotericin B-resistant clones.

Basal PM Cholesterol Esterification Assay—[^{3}H]Cholesterol (1 mCi/ml) was obtained from PerkinElmer (NET 139). [^{3}H]Cholesteryl ester formation was assessed as described previously (2). Cells were split from confluency by one-third and grown for 24 h. These cells were then seeded at 2.5×10^4 per well in a 6-well dish for 24 h. Medium was changed to 5% LPDS for 24 h. Cells were then pulsed for a given time with 1 μCi/ml [^{3}H]cholesterol in 1 ml of 5% LPDS media and were treated with either 1 μM 25-hydroxycholesterol in ethanol (final ethanol concentration, 0.01%) or 50 μM 2-hydroxypropyl-β-cyclodextrin-cholesterol where indicated. Cyclodextrin:cholesterol complexes were prepared as described in Lange *et al.* (21). Cells were washed with cold Tris-buffered saline (TBS) for 10 min at 4 °C. Lipids were extracted from each well in 3 ml of 3:2 hexane: isopropyl alcohol and dried under nitrogen. [^{14}C]Cholesteryl oleate was added to lipid extracts as a recovery standard. Cholesteryl esters (CE) were separated from cholesterol by thin layer chromatography (TLC) in a 130:30:2 heptane/ethyl ether/acetic acid solvent using 100 μg of cholesterol and 30 μg of CE as carriers, respectively, and visualized by iodine. The percentage of recovery of [^{3}H]CE was assessed by recovery of [^{14}C]cholesteryl oleate. [^{3}H]Cholesterol esterification was measured as a ratio of recovery-normalized [^{3}H]CE to total [^{3}H]cholesterol.

ACAT Activity Assays—Acyl-CoA:cholesterol acyltransferase (ACAT) activity was carried out as described previously (4). Cells were seeded at 5×10^5 in 10-cm plates overnight. Medium was changed to 5% LPDS for 24 h. Isolated microsomes were resuspended in 60 μl of 0.1 M potassium phosphate (pH 7.4)/1 mM DTT and supplemented with 1 mg of fatty acid-free BSA in 0.1 M K-phosphate/DTT buffer. For the ACAT activity assay, 100 μl of cholesterol/Triton WR-1339 solution (20 μg of cholesterol, 60 μg of Triton-WR) was added to provide excess cholesterol. 20 μl of 250 μM [^{14}C]oleoyl-CoA in 0.01 M K-phosphate was added to label CE formed by ACAT. ACAT inhibitor, CI-976 (gift from Warner-Lambert), dissolved in ethanol, was added to a 2 μM final concentration where described. Esterification was carried out at 37 °C for 15 min for ACAT activity and quenched with 4 ml of 2:1 chloroform/methanol. 800 μl of PBS was added to extract lipids, and organic phase was removed and dried down under nitrogen. CE were separated by TLC in the same manner as described above and counted by scintillation.

Electron Microscopy—Deep etch electron microscopy to assess plasma membrane-ER contact sites was performed in the Heuser laboratory (Washington University) as described (22). Cells were grown on coverslips and unroofed using a brief ultra-

sound pulse in an intracellular buffer (30 mM Hepes, pH 7.2, 70 mM KCL, 5 mM $MgCl_2$, and 3 mM EGTA). Samples were immediately fixed in buffer containing 4% paraformaldehyde or 2% glutaraldehyde. Coverslips were frozen, replicated, and imaged as described (22).

PM and ER Fractionations—Isolation of PM was carried out using the plasma membrane protein extraction kit per the manufacturer's protocol (Abcam, Cambridge, MA). Briefly, cells were seeded at a density of 3×10^5 per 10-cm plate and grown for 24 h in normal medium and then changed to medium containing 5% LPDS for 24 h. 50 plates were used for each fractionation. Cells were homogenized with 75 stokes in a Dounce homogenizer, and the postnuclear supernatant was spun at $10{,}000 \times g$ to obtain total cellular membrane proteins. Membranes were then resuspended in the upper phase solution and extracted using the lower phase solution followed by centrifugation to pellet the PM. ER membranes were isolated as described previously (23). Equal protein amounts of each fraction were run by SDS-PAGE and assessed for purity by Western blotting with Na/K^+ ATPase (sodium pump), protein disulfide isomerase, and prohibitin organelle markers for the PM, ER, and mitochondria, respectively.

Lipidomics—To membrane fractions, internal standards (either deuterated or incorporating odd chain fatty acyl species) were added, and lipid extraction was performed by the method of Bligh and Dyer (24). Liquid chromatography tandem mass spectrometry (LC-MS/MS) was used for lipid species quantification (25).

RACE—The exon sequence fused upstream of the ROSAβGEO cassette was identified by 5′ RACE (SMART RACE cDNA amplification kit, Clontech) of total RNA extracted from the CHO A1 cell line, utilizing the known sequences of a 5′-ligated oligonucleotide and the ROSAβGEO transcript (see supplemental Table 1). The resulting sequenced 5′ RACE product was then used to conduct 3′ RACE using wild type (WT) CHO RNA to identify the remaining 3′ exons in the disrupted locus. PCR was carried out using WT CHO or A1 genomic DNA as a template, with a forward primer specific to the 5′ end of the RACE product and a reverse primer either specific to the 3′ end of the RACE product to amplify the WT locus or specific to the middle of the ROSAβGEO provirus to amplify the disrupted locus.

Southern Blot—Genomic DNA from WT CHO and A1 cells were digested with XbaI, NotI, and BglII, run on a 1% agarose gel, and transferred to GeneScreen nylon membrane. A ^{32}P end-labeled probe antisense to the ROSAβGEO sequence was used to probe for ROSAβGEO proviral integration.

Generation of U60-complemented Clones and U60 Knockdown Clones—The full-length *U60snhg* mouse locus was amplified from genomic DNA. It contains 2 kb of upstream promoter sequence and 1 kb of sequence downstream of U60snhg exon 2. The PCR product was amplified with primers containing NotI and Kpn1 sequences for cloning into the pSilencer 4.1 vector lacking CMV. To generate stable knockdown clones, an shRNA oligonucleotide (see supplemental Table 1) directed against the murine U60snoRNA was cloned into a pSilencer 4.1-CMV Hygro vector (Ambion). The shRNA vector was transfected into NIH 3T3 cells. Cells were plated at limiting dilution and selected with hygromycin, and clonal cell lines (KD1 and KD2) were isolated.

Measurement of U60 snoRNA by qPCR—TRIzol-extracted RNA was reverse-transcribed with the SuperScript III kit (Invitrogen). U60 snoRNA was reverse-transcribed with a stem-loop primer with oligo(dT) reversed transcribed poly(A) RNAs. cDNAs were detected and amplified using SYBR Green master mix (Applied Biosciences) (see primer list in supplemental Table 1).

U60 snoRNA Immunoprecipitation—U60 snoRNA was *in vitro* transcribed from a short DNA oligonucleotide containing a 5′ T7 sequence and the mouse *SNORD60* gene (MEGAshortscript T7 kit, Invitrogen). The *in vitro* transcription reaction was run on an 8 M urea 10% polyacrylamide gel. RNA products were visualized by ethidium bromide staining and excised for overnight elution. Eluted U60 was precipitated and end-labeled with 3′-biotin (RNA 3′ end biotinylation kit, Pierce). The efficiency of labeling was determined by dot blot. 3T3 mouse fibroblasts were seeded and cultured overnight at 5×10^5 cells/10-cm plate. Cells were transfected with 5 pmol of Bio-U60 plus 8 μg of FLAG-protein DNA construct per plate using Lipofectamine Plus. Cells were lysed in TNEN (50 mM Tris, pH 8.0, 0.15 M NaCl, 2 mM EDTA, 0.5% Nonidet P-40, 1× Complete protease inhibitor cocktail, 1 mM PMSF) buffer plus Superasin 24 h after transfection, and postnuclear supernatant was used for FLAG immunoprecipitation using anti-FLAG beads (anti-FLAG M2 affinity gel, Sigma) (26). RNA was extracted from FLAG beads using TRIzol, and RNA was run on 4% native polyacrylamide gel, transferred to nylon membrane, and blotted for presence of biotin (chemiluminescent nucleic acid detection module, Pierce).

Measurement of Site-specific rRNA Methylation by Primer Extension qPCR—Detection of rRNA methylation was adapted from Belin *et al.* (27). RNA was extracted from yeast cells using the RiboPure-yeast kit (Ambion) or from CHO cell lines using TRIzol. 28 S and 18 S RNAs were separated from total RNA by agarose-gel electrophoresis, visualized by ethidium bromide staining, and isolated by gel extraction. One ng of rRNA was used for reverse transcription (RT) by SuperScript III in the presence of either 1 μM or 1 mM dNTPs using reverse primer directed downstream of the methylation site. qPCR was carried out using SYBR Green master mix to detect RT extended primers using the primer set flanking methylation site (supplemental Table 1).

RESULTS

Amphotericin B Loss-of-Function Screen—To generate a pool of mutagenized CHO cells, we performed insertional mutagenesis using the ROSAβGEO retrovirus (19, 20). Transduction was optimized to achieve an average of one insertion per 20 genomes. The integrated provirus contains a β-galactosidase gene, a neomycin resistance gene, and a poly(A) signal with no upstream promoter sequence, thus only conferring antibiotic resistance and genetic disruption if integrated downstream of an active promoter and splice donor. G418 selection of transduced cells was used to generate a pool of stably mutagenized CHO cells. This pool of cells was subjected to amphotericin B/LDL selection twice, after which individual cell lines were

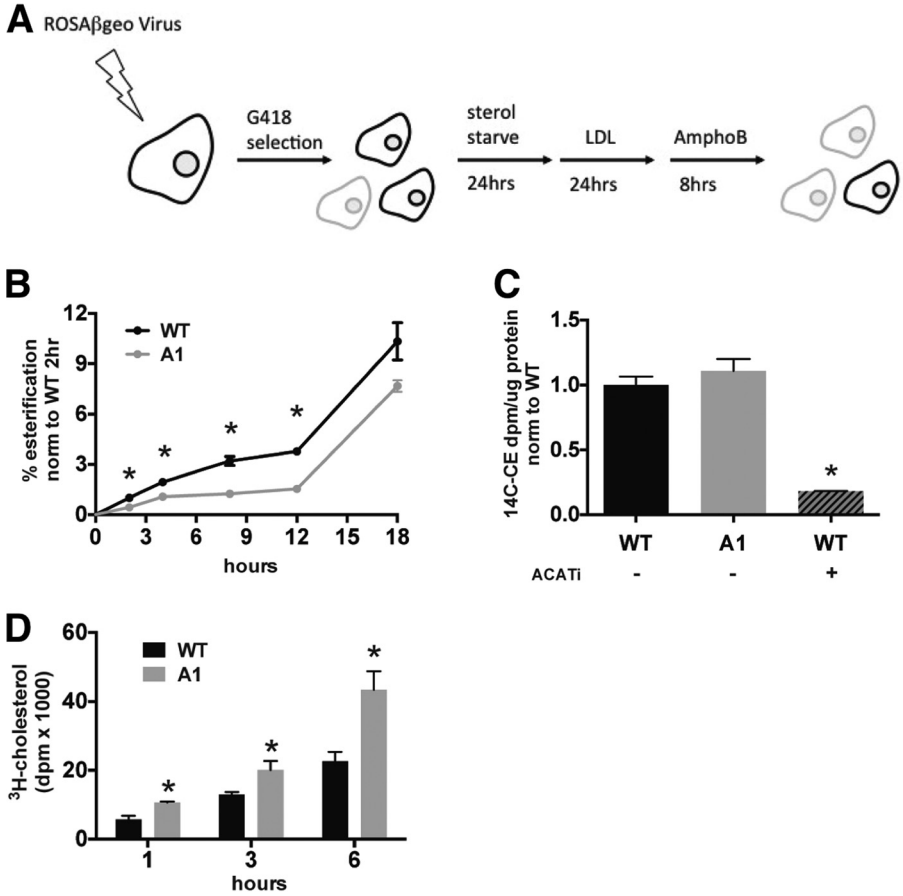

FIGURE 1. **The A1 mutant cell line displays decreased cholesterol trafficking to the ER.** *A*, amphotericin B loss-of-function screen. A pool of CHO cell mutants stably infected with the ROSAβGEO retrovirus was cholesterol-starved, treated with LDL cholesterol, and then selected in amphotericin B. *Gray cells* indicate those that did not survive either the G418 or amphotericin selection. *B–D*, CHO cell lines were seeded for 24 h in normal media and then cultured in LPDS media for 24 h. *B*, PM cholesterol esterification. Cells were pulsed with [^{3}H]cholesterol over a time course, total lipids were extracted, and the percentage of cholesterol esterification was calculated by scintillation counting of [^{3}H]CE and [^{3}H]cholesterol species. Data represent mean values $\pm$S.E. from triplicate cultures. *, $p < 0.05$ for A1 *versus* WT. *C*, ACAT activity. Microsomal fractions from cells were pulsed with [^{14}C]oleate and excess cholesterol. ACAT inhibitor was used for positive control. [^{14}C]CE were counted by scintillation. Data represent mean of triplicate cultures $\pm$S.E., $p < 0.005$ for WT plus ACAT inhibitor (*ACATi*) *versus* WT. *D*, cholesterol synthesis. Cells were pulsed with [^{3}H]acetate over a time course. [^{3}H]Cholesterol species were counted by scintillation. Data represent mean values $\pm$S.E. from triplicate cultures. *, $p < 0.05$ for A1 *versus* WT.

isolated (Fig. 1*A*). At the amphotericin B and LDL concentrations used in the screen, nonmutagenized WT cells failed to survive the two rounds of selection, thus minimizing background. To select amphotericin B-resistant mutants that did not simply harbor defects in the egress of endolysosomal cholesterol (*e.g.* NPC1 mutants), only clones that displayed normal filipin staining patterns (28) were selected for further analysis.

The A1 Mutant Cell Line Has Reduced PM to ER Cholesterol Trafficking—To screen CHO mutants for altered rates of cholesterol transfer from the PM to internal membranes, we measured the availability of PM cholesterol for trafficking to the ER by determining the rate of esterification of cell surface cholesterol by ACAT. For these experiments, cells were grown in lipoprotein-deficient medium, pulsed with ethanolic [^{3}H]cholesterol, which readily incorporates into the PM, and subsequently assayed for detection of [^{3}H]CE. One of the cell lines, A1, consistently displayed a 50–60% decrease in basal [^{3}H]CE formation over a 24-h time course when compared with WT cells (Fig. 1*B*). This was not due to a deficiency in ACAT activity in A1 as microsomes isolated from WT and A1 cells incubated with [^{14}C]oleate and excess cholesterol displayed similar levels of [^{14}C]CE formation (Fig. 1*C*). Because the cycling of cholesterol between the PM and ER is required for proper sensing of total cellular cholesterol levels by the ER-localized SREBP cleavage-activating protein (SCAP) and Insig sterol-sensing proteins, deficiency in PM to ER cholesterol trafficking in A1 cells would be expected to result in dysregulated cholesterol synthesis. Incorporation of [^{3}H]acetate into *de novo* synthesized cholesterol was measured in WT and A1 cells over a time course. Under the same growth conditions used for the basal cholesterol esterification assay, the A1 cell line displayed a 2-fold increase in the rate of cholesterol synthesis when compared with WT cells (Fig. 1*D*). Together with the basal PM cholesterol esterification assay, these data suggest that A1 cells, when grown in the absence of exogenous LDL cholesterol, are deficient in cholesterol trafficking from the PM to the ER.

To determine whether altered expression of genes previously implicated in regulation of cholesterol homeostasis might be contributing to the cholesterol trafficking phenotype (7, 10, 11), we measured the mRNA abundance of cholesterol trafficking genes (caveolin 1, *STARD4*, *ORP1S*, and *ORP2*) and plasmalogen synthesis genes (*DHAPAT* and *DHAPS*) using hamster-

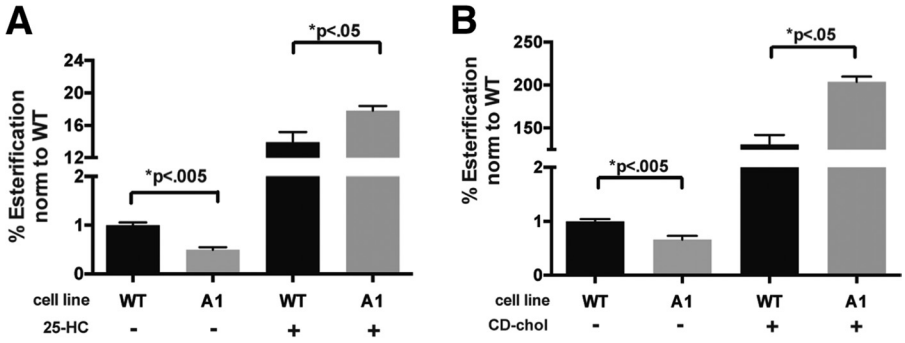

FIGURE 2. **Cholesterol activation corrects the PM to ER cholesterol trafficking defect in the A1 cell line.** *A* and *B*, cells were pulsed with [^{3}H]cholesterol and co-treated with either 25-hydroxycholesterol (*25-HC*) (*A*) or 2-hydroxypropyl-β-cyclodextrin-complexed cholesterol (*HPCD*) (*B*). The percentage of cholesterol esterification was calculated after scintillation counting of [^{3}H]CE and [^{3}H]cholesterol. Data represent mean values ±S.E. from triplicate cultures.

specific primers (supplemental Table 1) and qPCR. No differences were found between WT and A1 cells with respect to expression of these genes (not shown). Electron microscopy studies of WT and A1 cells were also performed but did not demonstrate differences in the density of PM-ER contact sites or in the morphology of PM caveolae (not shown).

Activation of PM Cholesterol Overcomes the Cholesterol Trafficking Defect in the A1 Mutant—The reduced PM to ER cholesterol trafficking in the A1 mutant could be a consequence of reduced PM cholesterol or altered membrane composition. In either event, reduced PM cholesterol activity, the tendency for cholesterol to leave the membrane, might be responsible for the trafficking defect. To test this, we treated cells with cholesterol-activating agents, 25-hydroxycholesterol or 2-hydroxypropyl-β-cyclodextrin-complexed cholesterol; both have been shown to stimulate esterification of PM-derived cholesterol by activating (*i.e.* stimulating the release) cholesterol in membranes (4). [^{3}H]CE formation was measured in WT and A1 cells treated with 25-hydroxycholesterol and 2-hydroxypropyl-β-cyclodextrin-complexed cholesterol, which stimulated esterification ~15–18-fold and ~150–200-fold above basal levels, respectively, in both cell lines. Interestingly, both treatments resulted in significantly greater [^{3}H]CE formation in A1 when compared with WT cells (Fig. 2, *A* and *B*). The increased formation of [^{3}H]CE demonstrates that not only is A1 PM cholesterol transfer to the ER intact under cholesterol-activating conditions, but cholesterol is actually transferred at a higher rate than in WT cells. These data would suggest that the A1 cholesterol trafficking defect does not result from PM cholesterol deficiency or defective cholesterol trafficking machinery.

A1 Cells Have Increased PM Phosphatidylcholine (LPC) Content—The dynamics of membrane-associated cholesterol are dependent on the composition of the resident lipid environment, in particular the phospholipid acyl chain composition (6, 29). To examine whether the A1 mutant has an altered cellular or PM lipidome that might affect movement of cholesterol within and between membranes, lipidomic analysis was performed on postnuclear supernatants and PM-enriched fractions from WT and A1 cells. Purity of PM fractions was assessed by detection of subcellular markers (Na/K^+ ATPase, PM; protein disulfide isomerase, ER; and prohibitin, mitochondria) through Western blotting and showed similar enrichment for the PM markers and depletion of the ER and mitochondrial markers in both parental and mutant cells (Fig. 3*A*). Using LC-MS/MS, the whole cell lysates and PM fractions from WT and A1 cells were broadly surveyed for cholesterol, cholesteryl ester, ceramide, sphingomyelin, phosphatidylcholine (PC), phosphatidylethanolamine, phosphatidylinositol, phosphatidylglycerol, and lysophosphatidylcholine (LPC) species. Total LPC species were increased 1.5-fold ($p < 0.05$) in the A1 PM fraction (Fig. 3*B*). This was principally attributable to an increase in the most abundant LPC species (LPC16:0) (Fig. 3*C*) and was accompanied by an ~1.6-fold ($p < 0.05$) increase in total saturation of LPC acyl chains. No significant differences were observed between WT and A1 cells in the other lipid classes (supplemental Fig. 1), although there was a trend toward increased PC 16:0/16:0 in the A1 PM fraction ($p = 0.07$) with a 1.2-fold increase in total saturation of PC acyl chains (Fig. 3, *D* and *E*).

The A1 Cell Line Is Haploinsufficient for Expression of the U60 snoRNA Host Gene—To identify the disrupted gene causing the cholesterol trafficking defect in the A1 cell line, we used the ROSAβGEO insertion as a tag to identify the locus of integration. Southern analysis probing for the ROSAβGEO proviral sequence revealed that the A1 cell line contains only one ROSAβGEO insertion (Fig. 4*A*). 5′ and 3′ RACE was conducted using RNA isolated from A1 to define the upstream exon sequence fused to the ROSAβGEO viral cassette and other exon sequences in the locus. BLAST analysis of the resulting 330-nucleotide RACE sequence against the mouse genome revealed no matching exon sequences (the hamster genome had not been sequenced at the time of this analysis). To confirm that the RACE sequence was produced from the locus of integration, PCR using forward and reverse primers designed to the 5′ and 3′ ends of the RACE sequence, respectively, was used to amplify the putative locus from WT and A1 genomic DNA. A single band was amplified from both WT and A1 templates. Using the same 5′ forward primer and a 3′ reverse primer designed to the ROSAβGEO cassette, a larger band was produced exclusively with A1 genomic template DNA, thus confirming that the RACE sequence corresponded to the locus disrupted by ROSAβGEO (Fig. 4*B*). That the smaller PCR product appeared using either WT or A1 template indicates that the A1 cell line also contains an intact WT locus and is likely to serve as a model of haploinsufficiency for the disrupted gene.

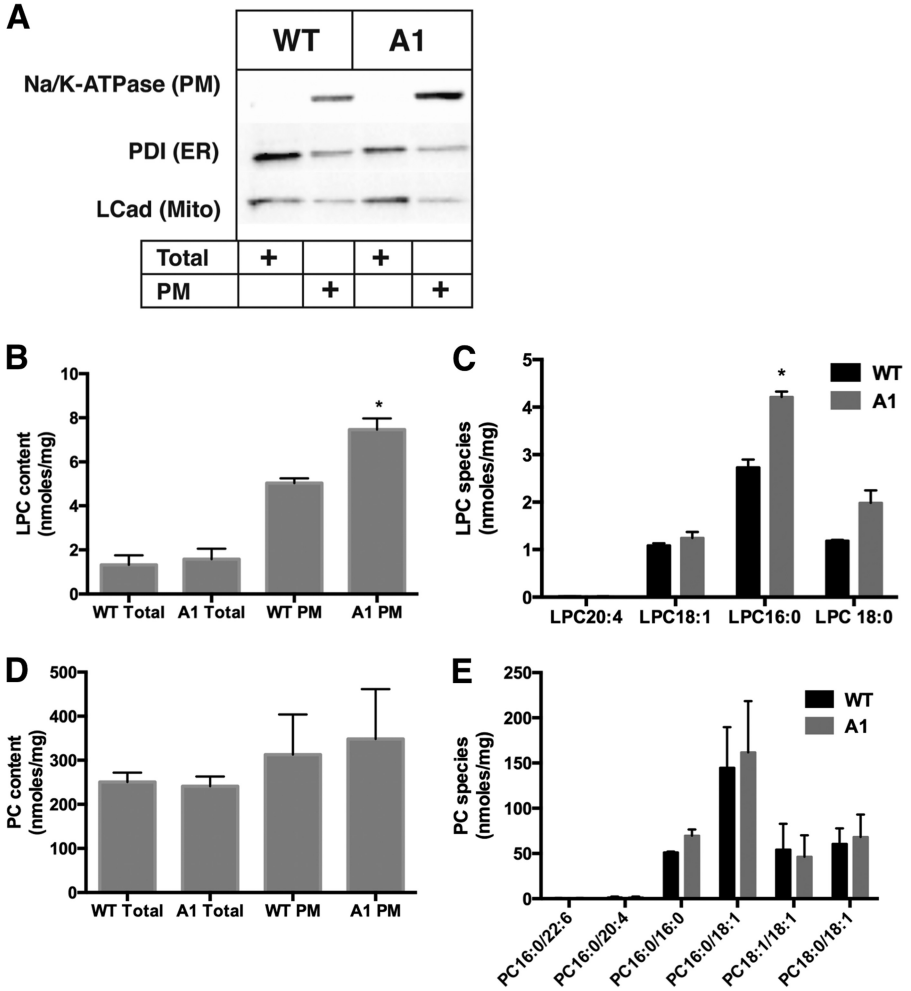

FIGURE 3. **LPC content is increased in PM in A1 cell line.** *A*, WT and A1 cells were seeded in normal medium for 24 h and then grown in LPDS for 24 h. Postnuclear supernatants and PM-enriched fractions were isolated from the WT and A1 cells. Purity was assessed by PM, ER, and mitochondrial (*Mito*) markers. *PDI*, protein disulfide isomerase; *LCad*, long chain acyl-CoA dehydrogenase. *B*, total LPC species are shown for postnuclear supernatants and PM fractions from WT and A1 cells. *, $p < 0.05$ for A1 *versus* WT. *C*, individual LPC species are shown for WT and A1 PM fractions. *, $p < 0.05$ for A1 *versus* WT. *D*, total PC species are shown for postnuclear supernatants and PM fractions from WT and A1 cells. *E*, individual PC species are shown for WT and A1 PM fractions. Data represent mean values ±S.E. and are representative of two independent experiments.

Because the initial RACE sequence did not contain significant homology to any known genome, these two PCR products were then sequenced to identify the locus of integration using other sequences of the gene and to determine the precise genomic locus at which ROSAβGEO integrated. BLAST analysis of these sequences revealed that the disrupted A1 locus was homologous to the mouse transcript 2610019E17Rik, also known as the U60 snoRNA host gene (*U60snhg*), which was identified by the highly conserved box C/D snoRNA, *snordU60*, within the intron of the gene.

Features of the U60snhg Locus and the U60 Box C/D snoRNA—U60snhg is comprised of two exons and one intron, generating an ~500-bp pre-mRNA transcript. The box C/D snoRNA U60 at the 5′ end of the *U60snhg* intron is the only region of significant sequence conservation in the gene (Fig. 4*C*). The exon-intron structure, however, is identical among all mammalian species. Additionally, the short promoter region (<500 bp) also contains areas of significant sequence homology, indicating that the *U60snhg* is likely to be similarly regulated at the transcriptional level among mammals. The *U60snhg* exon sequences in the mouse, rat, and human genomes contain no open reading frames, whereas the hamster sequence contains two predicted products of 36 and 44 amino acids that are not evolutionarily conserved, suggesting that *U60snhg* is, indeed, a noncoding RNA. Taking these data together, it seems likely that the main function of *U60snhg* is to serve as a transcriptional unit to generate the intron lariat housing U60 snoRNA for processing into a mature snoRNA.

The U60 snoRNA belongs to the box C/D class of snoRNAs. Similar to canonical box C/D snoRNAs, U60 contains box C (UGAUGA) and box D (CUGA) sequence elements on the 5′ and 3′ ends, respectively, with lesser conserved canonical internal box C′ and box D′ elements as well (Fig. 4*C*). The C and D box elements are necessary for the binding of the core proteins that recruit the fibrillarin methyltransferase to the snoRNP. C/D snoRNPs can then mediate 2′-*O*-methylation of rRNA nucleotides by bringing fibrillarin in close proximity to the targeted site via complementary base pairing between the snoRNA antisense element (ASE) and the rRNA sequence containing the nucleotide to be modified. U60 is thus predicted to base pair

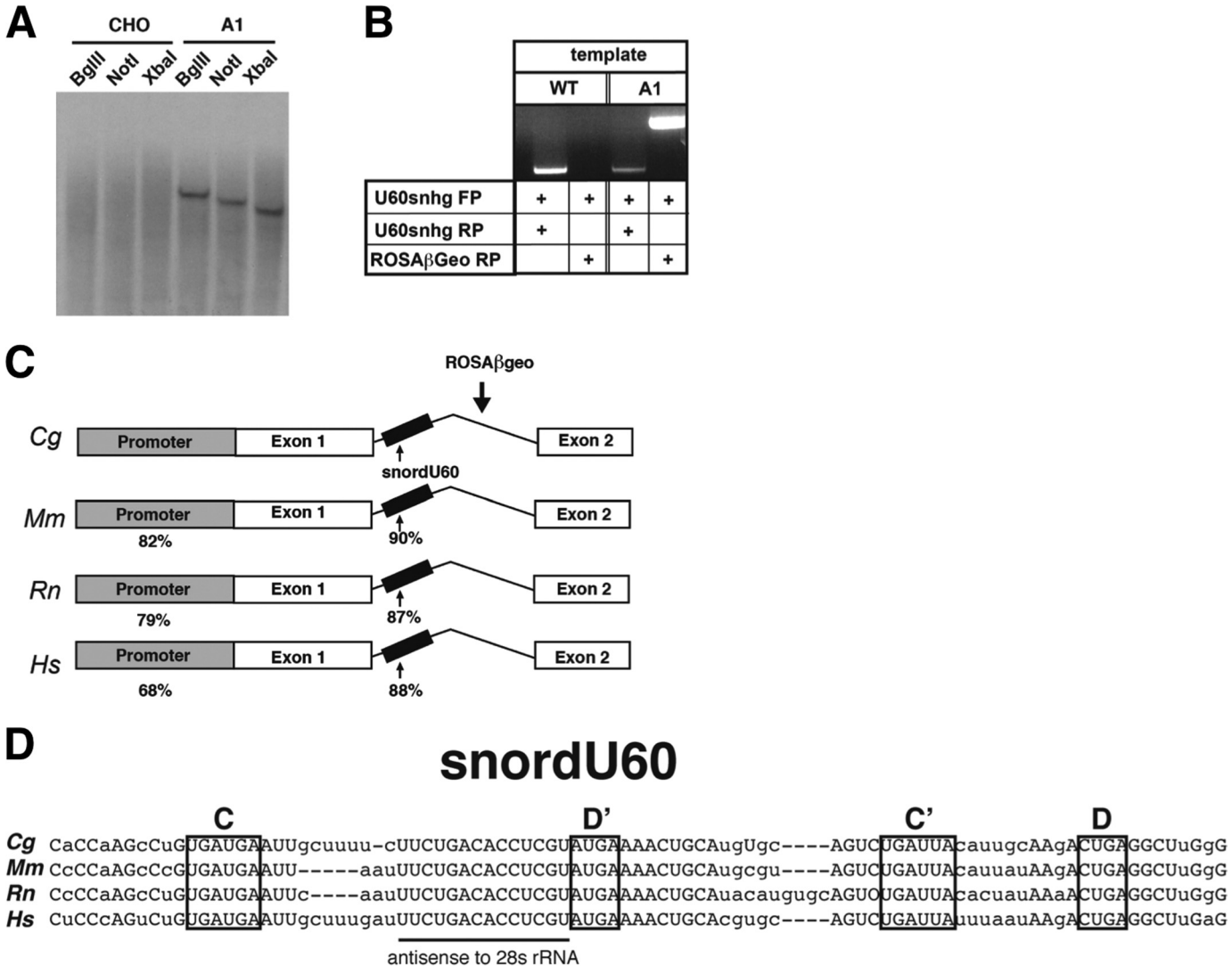

FIGURE 4. **The A1 cell line harbors a disrupted allele of the U60 snoRNA host gene.** *A*, Southern analysis using a ^{32}P-labeled ROSAβGEO probe was conducted on BglII, NotI, and XbaI fragmented genomic DNA from WT and A1 cell lines. *B*, directed PCR was used to verify locus of integration using WT or A1 genomic DNA as template. *FP*, forward primer; *RP*, reverse primer. *C*, depiction of structure of U60snhg gene in hamster (*Cg*) mouse (*Mm*), rat (*Rn*), and human (*Hs*) genomes. ROSAβGEO integration in A1 cell line indicated in hamster sequence. The percentages of conservation of promoter and snoRNA sequences are indicated. *D*, alignment of U60 snoRNA from hamster, mouse, rat, and human genomes. *Capital letters* indicate conserved nucleotides.

with 28 S rRNA via its ASE upstream of the D′ box and is thought to perform the 2′-*O*-methylation identified at nucleotide G4340.

Sequencing of the ROSAβGEO PCR product obtained using A1 genomic DNA as template revealed that integration of ROSAβGEO into this locus occurred within the *U60snhg* intron, downstream of the snoRNA and upstream of the branch point adenosine. It has been shown that the spacing between the 3′ end of intronic box C/D snoRNAs and the branch point is important for proper processing of such snoRNAs from intron lariat (30). Thus, improper processing of U60 at this disrupted locus in A1 would be expected to contribute to decreased levels of the mature U60 snoRNA.

The A1 Cell Line Is Haploinsufficient for U60 snoRNA Expression—RT-qPCR was used to detect mature U60 snoRNA levels. To ensure that the *U60snhg* pre-mRNA was not amplified in this method, a stem-loop primer for reverse transcription was designed to prime to the last 6 bp of the 3′ end of the processed U60 snoRNA. For qPCR, a conventional forward primer was directed to the 5′ end of U60 with a reverse primer directed to the denatured stem-loop primer. When compared with WT cells, a 50% reduction in mature U60 snoRNA levels was observed in A1 (Fig. 5*A*). Interestingly, growth of WT and A1 cells in lipoprotein-deficient serum appeared to suppress U60 snoRNA expression, suggesting that regulation of U60 snoRNA expression is responsive to cellular cholesterol content. As expected, disruption of one *U60snhg* allele in the A1 mutant results in U60 snoRNA haploinsufficiency.

The Cholesterol Trafficking Defect in A1 Mutant Is Abrogated by Complementation with U60 snoRNA—To determine whether reduced U60 snoRNA expression causes the A1 cell line cholesterol trafficking phenotype, A1 clones stably expressing the full-length mouse *U60snhg* genomic locus (A1-WT) were generated and screened for complementation by the basal PM cholesterol esterification assay. To express the U60 snoRNA at endogenous levels, 2 kb of upstream sequence was

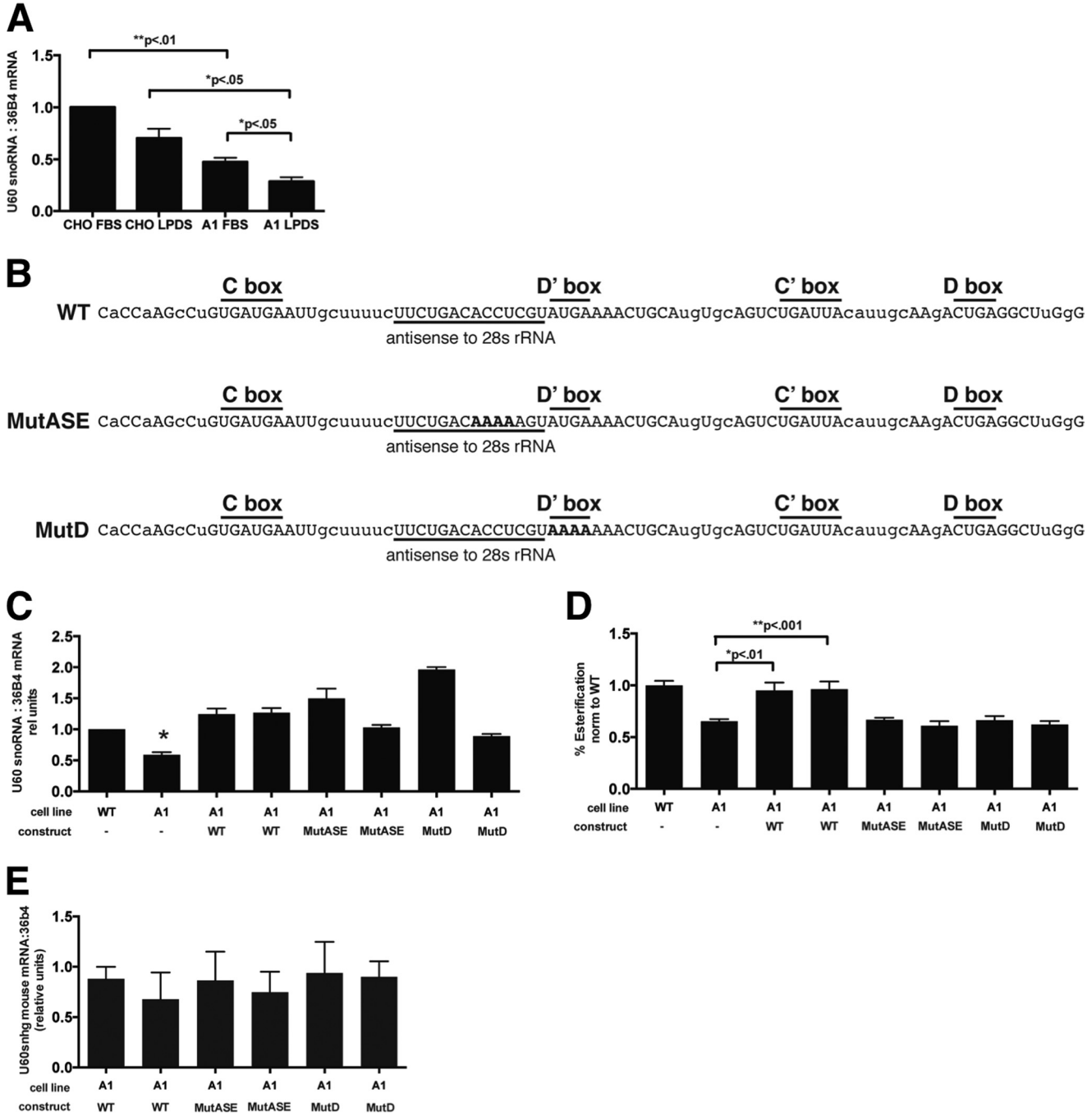

FIGURE 5. **Reduced U60 snoRNA expression causes reduced PM to ER cholesterol trafficking in the A1 cell line.** *A*, U60 snoRNA expression was measured by qPCR using a 3′-U60 specific stem-loop primer for RT and normalized to 36B4 mRNA. Data are represented as mean ± S.E. from three separate experiments. *B*, mouse U60snhg expression constructs WT, mutASE, and mutD used for complementation of A1 cell line in *C*. *Capital letters* indicate nucleotides conserved among mammalian species. *C*, stable cell lines were generated after transfection of A1 cells with indicated constructs and selection with hygromycin. Mouse U60 snoRNA expression was measured as in *A*. *, $p < 0.05$, **, $p < 0.01$ for A1 *versus* WT and all other clones. *rel units*, relative units. *D*, PM cholesterol esterification assay. cells were pulsed with [^{3}H]cholesterol for 4 h. Data represent mean esterification ±S.E., normalized to WT, from three separate experiments. *E*, expression of mouse U60snhg mRNA was measured by qPCR in complemented clones, normalized to 36B4 mRNA. Data represent mean values ±S.E. from triplicate cultures. Data values are not significantly different.

included as a promoter. Clones expressing the U60 snoRNA at levels greater than or equal to WT levels were chosen for complementation analysis (Fig. 5*C*). In two A1-WT clones, cholesterol esterification was restored to WT levels (Fig. 5*D*). To assess whether the U60 snoRNA or the *U60snhg* mRNA is the critical transcriptional unit in the locus, clones stably expressing the *U60snhg* locus in which the D′ box or a portion of the ASE of the U60 snoRNA were mutated to adenines (A1-D box or A1-ASE, Fig. 5*B*) and assayed for esterification. The D′ box is important for proper C/D snoRNP formation, whereas the ASE sequence, which is complementary to the U60 RNA target, 28 S rRNA, is predicted to direct site-specific methylation. None of the A1-D box or A1-ASE clones displayed cholesterol esterification levels significantly different from the A1 cell line, despite

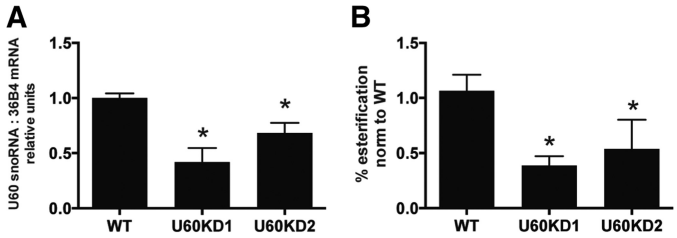

FIGURE 6. **Knockdown of U60 snoRNA recapitulates the A1 cholesterol trafficking defect in 3T3 mouse fibroblasts.** *A*, stable U60KD cell lines were generated after transfection with U60shRNA expression vector and selection with hygromycin. U60 snoRNA expression was measured by qPCR, normalized to 36B4 mRNA. Data represent mean expression ±S.E. from three separate experiments. *B*, PM cholesterol esterification assay. Cells were pulsed with [^{3}H]cholesterol for 4 h. Data represent mean values ±S.E. from triplicate cultures. *, $p < 0.05$ for U60KD *versus* WT. *norm*, normalized.

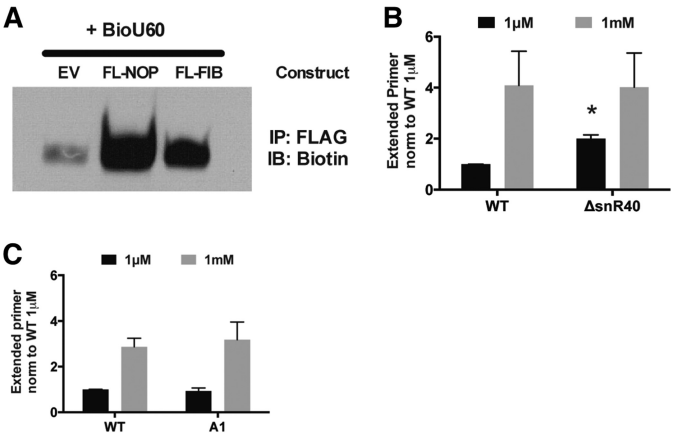

FIGURE 7. **Reduced U60 snoRNA expression does not affect U60 snoRNP-mediated rRNA methylation in the A1 cell line.** *A*, C/D snoRNP immunoprecipitation (*IP*). Streptavidin-HRP blot depicts BioU60 immunoprecipitated by anti-FLAG antibody following co-transfection of 3T3 cells with BioU60 and either empty vector (*EV*), FLAG-Nop56 (*FL-NOP*), or FLAG-Fibrillarin (*FL-FIB*). *IB*, immunoblot. *B*, primer extension qPCR. 18 S rRNA from WT or Δsnr40 yeast strains was used as template for primer extension at low and high dNTP concentrations to measure G1267 methylation. *norm*, normalized. *C*, 28 S rRNA isolated from CHO and A1 cells was used as template for primer extension to measure G4340 methylation. *B* and *C*, extended primers were detected by qPCR using primers flanking methylation site of interest. Data represent mean values ±S.E. from three separate experiments. *, $p < 0.05$ for Δsnr40 *versus* WT. *norm*, normalized.

having WT levels of U60 snoRNA expression. Importantly, the clones stably expressing these mutants showed equal *U60snhg* mRNA expression, ensuring that lack of complementation was not due to reduced expression of other elements in this locus (Fig. 5*D*). Taken together, these data indicate that not only is the U60 snoRNA the relevant transcriptional unit of the locus in affecting PM to ER cholesterol trafficking, but the data also indicate that the D′ box and the antisense element are necessary for this function of U60.

U60 snoRNA Knockdown Recapitulates Cholesterol Trafficking Defect in 3T3 Mouse Fibroblasts—To determine whether reduced U60 expression can affect PM cholesterol trafficking in other cell types, we knocked down the U60 snoRNA in mouse 3T3 fibroblasts. In two clones stably expressing an shRNA directed to knock down U60, reduced U60 expression caused a decrease in basal PM cholesterol esterification (Fig. 6). Thus, recapitulation of the A1 cell line cholesterol trafficking defect in another organism and cell line confirms that the U60 snoRNA likely functions to affect PM cholesterol trafficking in mammalian cells.

The U60 snoRNA Associates with Canonical C/D snoRNP Core Proteins—As a putative box C/D snoRNA, we first sought to verify that U60 is capable of forming a C/D snoRNP. To accomplish this, RNA immunoprecipitation was used to detecting a 3′ end biotin-labeled U60 snoRNA (BioU60) within C/D snoRNP immunoprecipitates. FLAG-Nop56 or FLAG-Fibrillarin constructs were co-expressed with BioU60 in 3T3 fibroblasts. Cells were lysed to perform FLAG immunoprecipitation from which RNA was extracted and probed for BioU60 content. BioU60 was shown to co-immunoprecipitate with both fibrillarin and Nop56 proteins (Fig. 7*A*), indicating that the U60 snoRNA can be reconstituted into a C/D snoRNP *in situ* and is likely to function as a canonical box C/D snoRNA.

Haploinsufficiency of the U60 snoRNA Does Not Cause Reduced 28 S rRNA G4340 Methylation—Although the methylation of ribosomal RNA has not been demonstrated to specifically affect cholesterol trafficking, we considered that decreased U60 expression could cause reduced G4340 methylation in the A1 cell line, which in turn might be responsible for the cholesterol trafficking phenotype. To test this, primer extension was used in conjunction with qPCR (27). In this method, RT is performed using rRNA as a template, with a reverse primer directed 50–100 bp downstream of the methylation site of interest. When carried out with low dNTP concentrations, the transcriptase will stall at methylated nucleotides. The extended primers are then detected by traditional qPCR methods, using a primer set directly flanking the methylation site. Increased levels of fully extended primer measured by qPCR, therefore, indicate decreased methylation. As a positive control, rRNA was isolated from WT and Δsnr40 knockout yeast strains, the latter containing no box C/D snr40 snoRNA and incapable of rRNA methylation at G1267 (31). When using Δsnr40 rRNA as a template for RT with low dNTPs, we observed that the reaction produced more extended primer than WT rRNA template (Fig. 7*B*). We then probed for G4340 methylation using WT and A1 28 S rRNA as template. qPCR detection of the RT-extended primer was equal in both samples (Fig. 7*C*). Although these data do not specifically address whether U60, in fact, methylates G4340, it does indicate that the methylation status of its only predicted target site is not affected by U60 haploinsufficiency in the A1 cell line. These data support the conclusion that the A1 mutant phenotype is not caused by defective rRNA methylation, and instead U60 acts by a noncanonical mechanism to affect cholesterol trafficking.

DISCUSSION

In the present study, we have identified a novel pathway linking a box C/D snoRNA to cholesterol homeostasis. We show that haploinsufficiency of the U60 snoRNA resulted in decreased PM to ER cholesterol trafficking, as measured by reduced PM cholesterol esterification and increased *de novo* cholesterol synthesis. This trafficking defect was overcome by complementation with the mouse U60snhg locus, whereas point mutations in the snoRNA sequence itself abrogated the complementation with this locus. These findings not only

implicate the snoRNA as the element of the locus that affects cholesterol trafficking, but also indicate that the regions within the snoRNA targeted for mutagenesis are necessary for this role of the U60 snoRNA. In demonstrating the ability of U60 to bind canonical C/D snoRNP core proteins, we found that U60 site-specific methylation was not deficient in the U60 haploinsufficient A1 cell line. Our findings demonstrate an unexpected role for the U60 snoRNA in regulation of intracellular cholesterol trafficking in a manner beyond its predicted canonical function.

Our studies suggest that the cholesterol trafficking defect in the amphotericin B-resistant A1 cell line is not simply a result of PM cholesterol deficiency as lipidomic analysis indicated normal PM cholesterol content and activation of PM cholesterol led to higher rates of cholesterol esterification than even WT cells. Instead, we speculate that under basal conditions, reduced propensity of cholesterol to leave the PM may responsible for the reduced PM cholesterol esterification. The cholesterol activation hypothesis (6) posits that the tendency of PM cholesterol to become more exposed at the aqueous-membrane interface and thereby increase accessibility to extramembrane acceptors is dependent on the lipid composition of the membrane. Increased saturation of PM phospholipid acyl chains could account for increased PM cholesterol retention: the saturated acyl chains interacting more strongly with cholesterol and positioning cholesterol closer to the bilayer center, thereby shielding cholesterol's hydroxyl group from interaction with extracellular membrane acceptors (6, 23, 29, 32). How reduced U60 expression might specifically alter the PM lipid environment will require further understanding of the noncanonical functions of the U60 snoRNA.

Although box C/D snoRNAs have previously been shown to mediate rRNA methylation in eukaryotic cells (31), much of this analysis has been conducted in lower eukaryotes that do not contain a highly conserved *U60snhg* homolog with requisite box C and box D snoRNA elements or with similar exon-intron structure (*Xenopus laevis*, *Gallus gallus*, lizards). Although rRNA methylation may be the sole function of the box C/D snoRNAs expressed in these lower organisms, the conservation of mammalian U60 supports the notion that it may have additional, unique function(s) in higher organisms. Recently, another forward genetics screen conducted by our laboratory designed to identify genes involved in lipotoxicity produced a mutant CHO cell line haploinsufficient for the four box C/D snoRNAs derived from the introns of the *rpL13a* locus (33). Similar to our current findings, this study demonstrated that reduced expression of the U32, U33, and U35 snoRNAs did not result in deficient rRNA methylation at the predicted nucleotides. Together with the current study, these findings suggest that haploinsufficiency of these snoRNAs is sufficient to achieve normal levels of rRNA methylation, yet renders the cells either resistant to metabolic stress, in the case of the *rpL13a* snoRNAs, or defective in cholesterol trafficking, in the case of the U60 snoRNA.

Indeed, a growing number of box C/D snoRNAs have been shown in recent studies to exhibit noncanonical functions, including serving as substrates for processing into smaller, microRNA-like species and targeting pre-mRNAs in ways that impact splicing (34, 35). A U60-derived microRNA-sized species (the first 21–22 nucleotides of the 5′ end of the snoRNA) is present in deep sequencing databases and was shown to be well represented in skin tissue (36). It seems unlikely, however, that this portion of the U60 snoRNA possesses microRNA function as the alignment of this sequence across mammalian species reveals poor conservation, and Custom TargetScan analysis reveals no common mRNA-3′-UTR targets across species. Abundance of this short sequence may possibly reflect a long-lived degradation product. As with other snoRNA roles, it is likely that U60 exerts its effects on another RNA(s) via an RNA-RNA complementarity. It is probable that U60 utilizes its highly conserved antisense element for such a function because we found this sequence to be required to support normal cholesterol trafficking. Future studies will focus on identification of such putative RNA targets.

In addition to the classical transcriptional mechanisms that regulate cholesterol levels, another class of noncoding RNAs has recently been demonstrated to function at several levels of cholesterol homeostasis. miR-33 has been shown to regulate *ABCA1*, *ABCG1*, and *NPC1* transcripts via 3′-UTR targeting, whereas the levels of miR-33 itself are also responsive to cellular cholesterol levels (37–39). These studies have established precedence for the role of noncoding RNAs in cholesterol biology, and we hypothesize that U60 may directly interact with other RNAs that play a role in cholesterol metabolism. In support of this notion, lowering intracellular cholesterol levels reduced U60 snoRNA expression, suggesting that either U60 expression or its stability is responsive to cellular cholesterol status. Moreover, the U60snhg promoter has been shown to be occupied by SREBP1 and its co-regulator NFY in HepG2 cells, indicating a potential for regulation by a cholesterol-responsive transcriptional program (40). Although most classical cholesterol-responsive genes are known to be transcriptionally activated under low cholesterol conditions, SREBP has also been demonstrated to transcriptionally repress genes involved in lipid catabolism, such as cholesterol 7α-hydroxylase (41). Beyond transcriptional and classical microRNA-mediated mechanisms, our study identifies snoRNAs as a new class of noncoding RNAs that contribute to regulation of cholesterol homeostasis.

Acknowledgments—We thank Robyn Roth and John Heuser for assistance with electron microscopy experiments. Mass spectrometry analyses were performed in the Metabolomics Facility at Washington University (National Institutes of Health Grant P30 DK020579).

REFERENCES

1. Kennedy, B. E., Charman, M., and Karten, B. (2012) Niemann-Pick Type C2 protein contributes to the transport of endosomal cholesterol to mitochondria without interacting with NPC1. *J. Lipid Res.* **53,** 2632–2642
2. Underwood, K. W., Jacobs, N. L., Howley, A., and Liscum, L. (1998) Evidence for a cholesterol transport pathway from lysosomes to endoplasmic reticulum that is independent of the plasma membrane. *J. Biol. Chem.* **273,** 4266–4274
3. Urano, Y., Watanabe, H., Murphy, S. R., Shibuya, Y., Geng, Y., Peden, A. A., Chang, C. C., and Chang, T. Y. (2008) Transport of LDL-derived cholesterol from the NPC1 compartment to the ER involves the trans-Golgi network and the SNARE protein complex. *Proc. Natl. Acad. Sci. U.S.A.* **105,** 16513–16518

4. Lange, Y., Ye, J., Rigney, M., and Steck, T. L. (1999) Regulation of endoplasmic reticulum cholesterol by plasma membrane cholesterol. *J. Lipid Res.* **40,** 2264–2270
5. Chang, T. Y., Chang, C. C., Ohgami, N., and Yamauchi, Y. (2006) Cholesterol sensing, trafficking, and esterification. *Annu. Rev. Cell Dev. Biol.* **22,** 129–157
6. Lange, Y., and Steck, T. L. (2008) Cholesterol homeostasis and the escape tendency (activity) of plasma membrane cholesterol. *Prog. Lipid Res.* **47,** 319–332
7. Munn, N. J., Arnio, E., Liu, D., Zoeller, R. A., and Liscum, L. (2003) Deficiency in ethanolamine plasmalogen leads to altered cholesterol transport. *J. Lipid Res.* **44,** 182–192
8. Yamauchi, Y., Reid, P. C., Sperry, J. B., Furukawa, K., Takeya, M., Chang, C. C., and Chang, T. Y. (2007) Plasma membrane rafts complete cholesterol synthesis by participating in retrograde movement of precursor sterols. *J. Biol. Chem.* **282,** 34994–35004
9. Baumann, N. A., Sullivan, D. P., Ohvo-Rekilä, H., Simonot, C., Pottekat, A., Klaassen, Z., Beh, C. T., and Menon, A. K. (2005) Transport of newly synthesized sterol to the sterol-enriched plasma membrane occurs via nonvesicular equilibration. *Biochemistry* **44,** 5816–5826
10. Jansen, M., Ohsaki, Y., Rita Rega, L., Bittman, R., Olkkonen, V. M., and Ikonen, E. (2011) Role of ORPs in sterol transport from plasma membrane to ER and lipid droplets in mammalian cells. *Traffic* **12,** 218–231
11. Mesmin, B., Pipalia, N. H., Lund, F. W., Ramlall, T. F., Sokolov, A., Eliezer, D., and Maxfield, F. R. (2011) STARD4 abundance regulates sterol transport and sensing. *Mol. Biol. Cell* **22,** 4004–4015
12. Schulz, T. A., Choi, M. G., Raychaudhuri, S., Mears, J. A., Ghirlando, R., Hinshaw, J. E., and Prinz, W. A. (2009) Lipid-regulated sterol transfer between closely apposed membranes by oxysterol-binding protein homologues. *J. Cell Biol.* **187,** 889–903
13. Dahl, N. K., Daunais, M. A., and Liscum, L. (1994) A second complementation class of cholesterol transport mutants with a variant Niemann-Pick type C phenotype. *J. Lipid Res.* **35,** 1839–1849
14. Dahl, N. K., Reed, K. L., Daunais, M. A., Faust, J. R., and Liscum, L. (1992) Isolation and characterization of Chinese hamster ovary cells defective in the intracellular metabolism of low density lipoprotein-derived cholesterol. *J. Biol. Chem.* **267,** 4889–4896
15. Jacobs, N. L., Andemariam, B., Underwood, K. W., Panchalingam, K., Sternberg, D., Kielian, M., and Liscum, L. (1997) Analysis of a Chinese hamster ovary cell mutant with defective mobilization of cholesterol from the plasma membrane to the endoplasmic reticulum. *J. Lipid Res.* **38,** 1973–1987
16. Wojtanik, K. M., and Liscum, L. (2003) The transport of low density lipoprotein-derived cholesterol to the plasma membrane is defective in NPC1 cells. *J. Biol. Chem.* **278,** 14850–14856
17. Gale, S. E., Westover, E. J., Dudley, N., Krishnan, K., Merlin, S., Scherrer, D. E., Han, X., Zhai, X., Brockman, H. L., Brown, R. E., Covey, D. F., Schaffer, J. E., Schlesinger, P., and Ory, D. S. (2009) Side chain oxygenated cholesterol regulates cellular cholesterol homeostasis through direct sterol-membrane interactions. *J. Biol. Chem.* **284,** 1755–1764
18. Olsen, B. N., Schlesinger, P. H., Ory, D. S., and Baker, N. A. (2011) 25-Hydroxycholesterol increases the availability of cholesterol in phospholipid membranes. *Biophys. J.* **100,** 948–956
19. Borradaile, N. M., Han, X., Harp, J. D., Gale, S. E., Ory, D. S., and Schaffer, J. E. (2006) Disruption of endoplasmic reticulum structure and integrity in lipotoxic cell death. *J. Lipid Res.* **47,** 2726–2737
20. Friedrich, G., and Soriano, P. (1991) Promoter traps in embryonic stem cells: a genetic screen to identify and mutate developmental genes in mice. *Genes Dev.* **5,** 1513–1523
21. Lange, Y., Ory, D. S., Ye, J., Lanier, M. H., Hsu, F. F., and Steck, T. L. (2008) Effectors of rapid homeostatic responses of endoplasmic reticulum cholesterol and 3-hydroxy-3-methylglutaryl-CoA reductase. *J. Biol. Chem.* **283,** 1445–1455
22. Hanson, P. I., Roth, R., Lin, Y., and Heuser, J. E. (2008) Plasma membrane deformation by circular arrays of ESCRT-III protein filaments. *J. Cell Biol.* **180,** 389–402
23. Sokolov, A., and Radhakrishnan, A. (2010) Accessibility of cholesterol in endoplasmic reticulum membranes and activation of SREBP-2 switch abruptly at a common cholesterol threshold. *J. Biol. Chem.* **285,** 29480–29490
24. Bligh, E. G., and Dyer, W. J. (1959) A rapid method of total lipid extraction and purification. *Can. J. Biochem. Physiol.* **37,** 911–917
25. Fan, M., Sidhu, R., Fujiwara, H., Tortelli, B., Zhang, J., Davidson, C., Walkley, S. U., Bagel, J. H., Vite, C., Yanjanin, N. M., Porter, F. D., Schaffer, J. E., and Ory, D. S. (2013) Identification of Niemann-Pick C1 disease biomarkers through sphingolipid profiling. *J. Lipid Res.* **54,** 2800–2814
26. Lewis, S. E., Listenberger, L. L., Ory, D. S., and Schaffer, J. E. (2001) Membrane topology of the murine fatty acid transport protein 1. *J. Biol. Chem.* **276,** 37042–37050
27. Belin, S., Beghin, A., Solano-Gonzàlez, E., Bezin, L., Brunet-Manquat, S., Textoris, J., Prats, A. C., Mertani, H. C., Dumontet, C., and Diaz, J. J. (2009) Dysregulation of ribosome biogenesis and translational capacity is associated with tumor progression of human breast cancer cells. *PLoS One* **4,** e7147
28. Millard, E. E., Srivastava, K., Traub, L. M., Schaffer, J. E., and Ory, D. S. (2000) Niemann-pick type C1 (NPC1) overexpression alters cellular cholesterol homeostasis. *J. Biol. Chem.* **275,** 38445–38451
29. Olsen, B. N., Bielska, A. A., Lee, T., Daily, M. D., Covey, D. F., Schlesinger, P. H., Baker, N. A., and Ory, D. S. (2013) The structural basis of cholesterol accessibility in membranes. *Biophys. J.* **105,** 1838–1847
30. Hirose, T., and Steitz, J. A. (2001) Position within the host intron is critical for efficient processing of box C/D snoRNAs in mammalian cells. *Proc. Natl. Acad. Sci. U.S.A.* **98,** 12914–12919
31. Lowe, T. M., and Eddy, S. R. (1999) A computational screen for methylation guide snoRNAs in yeast. *Science* **283,** 1168–1171
32. Lange, Y., Tabei, S. M., Ye, J., and Steck, T. L. (2013) Stability and stoichiometry of bilayer phospholipid-cholesterol complexes: Relationship to cellular sterol distribution and homeostasis. *Biochemistry* **52,** 6950–6959
33. Michel, C. I., Holley, C. L., Scruggs, B. S., Sidhu, R., Brookheart, R. T., Listenberger, L. L., Behlke, M. A., Ory, D. S., and Schaffer, J. E. (2011) Small nucleolar RNAs U32a, U33, and U35a are critical mediators of metabolic stress. *Cell Metab.* **14,** 33–44
34. Brameier, M., Herwig, A., Reinhardt, R., Walter, L., and Gruber, J. (2011) Human box C/D snoRNAs with miRNA like functions: expanding the range of regulatory RNAs. *Nucleic Acids Res.* **39,** 675–686
35. Kishore, S., Khanna, A., Zhang, Z., Hui, J., Balwierz, P. J., Stefan, M., Beach, C., Nicholls, R. D., Zavolan, M., and Stamm, S. (2010) The snoRNA MBII-52 (SNORD 115) is processed into smaller RNAs and regulates alternative splicing. *Hum. Mol. Genet.* **19,** 1153–1164
36. Xia, J., Joyce, C. E., Bowcock, A. M., and Zhang, W. (2013) Noncanonical microRNAs and endogenous siRNAs in normal and psoriatic human skin. *Hum. Mol. Genet.* **22,** 737–748
37. Marquart, T. J., Allen, R. M., Ory, D. S., and Baldán, A. (2010) miR-33 links SREBP-2 induction to repression of sterol transporters. *Proc. Natl. Acad. Sci. U.S.A.* **107,** 12228–12232
38. Najafi-Shoushtari, S. H., Kristo, F., Li, Y., Shioda, T., Cohen, D. E., Gerszten, R. E., and Näär, A. M. (2010) MicroRNA-33 and the SREBP host genes cooperate to control cholesterol homeostasis. *Science* **328,** 1566–1569
39. Rayner, K. J., Sheedy, F. J., Esau, C. C., Hussain, F. N., Temel, R. E., Parathath, S., van Gils, J. M., Rayner, A. J., Chang, A. N., Suarez, Y., Fernandez-Hernando, C., Fisher, E. A., and Moore, K. J. (2011) Antagonism of miR-33 in mice promotes reverse cholesterol transport and regression of atherosclerosis. *J. Clin. Invest.* **121,** 2921–2931
40. Reed, B. D., Charos, A. E., Szekely, A. M., Weissman, S. M., and Snyder, M. (2008) Genome-wide occupancy of SREBP1 and its partners NFY and SP1 reveals novel functional roles and combinatorial regulation of distinct classes of genes. *PLoS Genet.* **4,** e1000133
41. Norlin, M., and Chiang, J. Y. (2004) Transcriptional regulation of human oxysterol 7α-hydroxylase by sterol response element binding protein. *Biochem. Biophys. Res. Commun.* **316,** 158–164